


RESEARCH

Open Access



# Optimization and characterization of exopolysaccharides from *Leuconostoc citreum* BH10 and its functional properties *in vitro*

Zhiwen Ge<sup>1,2</sup>, Fidelis Azi<sup>2</sup>, Xuan Bao<sup>2</sup>, Xintao Yin<sup>2</sup>, Xue Feng<sup>2</sup>, Min Zhang<sup>2</sup>, Xiudong Xia<sup>1,3\*</sup> and Mingsheng Dong<sup>2\*</sup> 

## Abstract

In this study, the yield of exopolysaccharides (LCEPS) produced by *Leuconostoc citreum* BH10 was optimized through the improvement of fermentation conditions. A three-level four-factor central composite design coupled with response surface methodology was employed to elucidate the interactions among four design variables, namely fermentation time ( $X_1$ ), fermentation temperature ( $X_2$ ), sucrose concentration ( $X_3$ ), and inoculation amount ( $X_4$ ) over a broad range of process conditions and determine their effects on LCEPS production. Based on the developed models, under the optimum process conditions of 49.99 h, 25.59 °C, 21.66, and 3.00%, the obtained maximum production of LCEPS was up to 55.96 g/L. Besides, the produced LCEPS presented better thermal stability than the original dextran and rendered finely emulsifying properties compared with commercial emulsifiers. Moreover, the LCEPS possessed good antioxidant activities and showed certain biofilm inhibition against *Staphylococcus aureus* ATCC 6538 strain, which indicated that it has fine potential to be used as an excellent additive into the food industry.

**Keywords** Exopolysaccharides, *Leuconostoc citreum* BH10, Response surface methodology, Emulsifying property, Antibiofilm activities

\*Correspondence:

Xiudong Xia

86084056@163.com

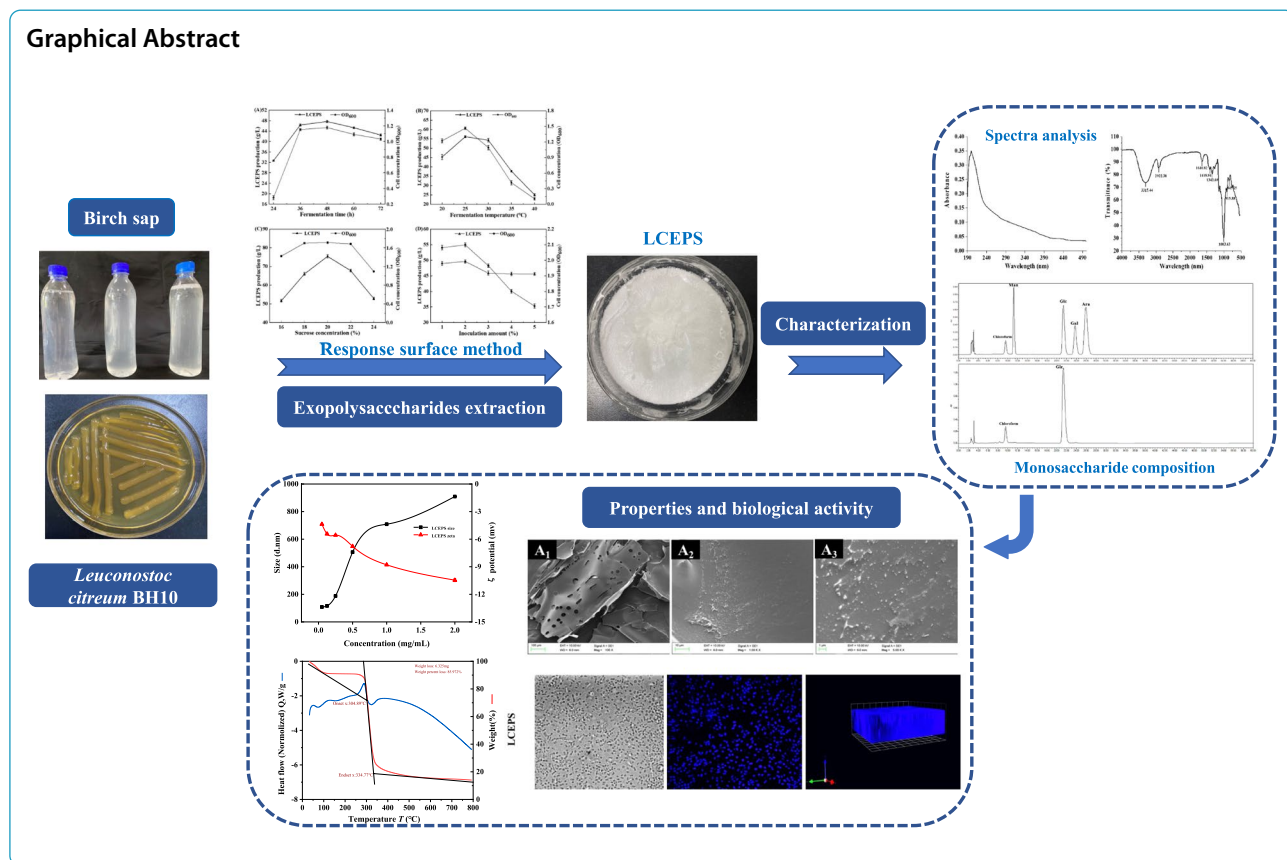
Mingsheng Dong

dongms@njau.edu.cn

Full list of author information is available at the end of the article



© The Author(s) 2023. **Open Access** This article is licensed under a Creative Commons Attribution 4.0 International License, which permits use, sharing, adaptation, distribution and reproduction in any medium or format, as long as you give appropriate credit to the original author(s) and the source, provide a link to the Creative Commons licence, and indicate if changes were made. The images or other third party material in this article are included in the article's Creative Commons licence, unless indicated otherwise in a credit line to the material. If material is not included in the article's Creative Commons licence and your intended use is not permitted by statutory regulation or exceeds the permitted use, you will need to obtain permission directly from the copyright holder. To view a copy of this licence, visit <http://creativecommons.org/licenses/by/4.0/>.



**Introduction**

Birch is one of the important tree species in northern China, possessing high environmental protection and economic value. The milky saps produced inside its tree cortex present weakly acidic ( $\text{pH } 4.3 \pm 0.1$ ) and contain active substances, such as betulin alcohol, polysaccharide, saponin, protein and minerals, and a variety of fructose, amino acid, vitamin and bioelement that human body needs, etc., and to be worldwide recognized as the nutritious, drinkable, physiologically active water containing rich nutrition (Kallio & Ahtonen 1987). It has medicinal value to human skin whitening, moisturizing, spot, and acne. Besides, it has anti-fatigue, anti-aging health-care function and can help to prevent the diseases of hypertension, heart disease, cancer, cerebral hemorrhage, and also can be used to treat gout, kidney stones, and scurvy, etc. (Enescu 2017).

Some previous studies reported that birch sap’s rich polysaccharides were closely related to its endophytic bacteria. The main endophytic bacteria of birch sap were mainly found to be *Leuconostoc*, and *Leuconostoc citreum* accounted for the most. *Leu. citreum* is a lactic

acid and gram-positive bacteria that can produce polysaccharides, lactate, bacteriocin and other metabolites (Abid et al. 2020). Dextran is a glucose polymer formed by D-glucose bonding through a glycosidic bond. Presently, most dextran applied in commercial utilization mainly comes from *Leu. mesenteroides*, whereas the comparative studies on the polysaccharide of *Leu. citreum* are few (Wang et al. 2019).

In this study, response surface optimization was performed on the polysaccharide-producing conditions of *Leu. citreum* BH10 which discovered in birch sap and collected from Hulunbuir City, Inner Mongolia Autonomous Region, China. The physicochemical properties of the produced polysaccharides were studied by gel permeation chromatography (GPC), high-performance liquid chromatography (HPLC), Fourier-transform infrared spectroscopy (FT-IR), ultraviolet-visible (UV-vis), scanning electron microscope (SEM) and thermogravimetric analysis (TGA), and its emulsifying, antioxidant properties and anti-biofilm activities in vitro were investigated, aiming to provide a theoretical basis for its application in the field of food industrialization.

## Materials and methods

### Materials

The monosaccharide standard (mannose, glucose, galactose and arabinose) and 3-methyl-1-phenyl-2-pyrazolin-5-one (PMP) were purchased from Aladdin Biotechnology Limited Co., Ltd. (Shanghai, China). The dialysis bag (Mw cutoff 8000–14,000 Da) and T-series dextran (T-10, T-50, T-100, T-200 and T-500) were obtained from Solarbio Life Science Co., Ltd. (Beijing, China). The vitamin C (VC), 1,1-diphenyl-2-picryl-hydrazyl (DPPH), 1,10-phenanthroline, nitro blue tetrazolium (NBT), nicotinamide adenine dinucleotide (NADH) and phenazine metho-sulfate (PMS) were obtained from McLean Biochemical Technology Co., Ltd. (Shanghai, China). The foodborne pathogen *Staphylococcus aureus* ATCC 6538 was obtained from Collaborative Innovation Center for meat production and processing, Jiangsu province, China. All other reagents were in analytical grade.

### Microorganism and culture medium

The newly isolated *Leu. citreum* BH10 strain was identified by 16S rRNA sequencing and stored at  $-20^{\circ}\text{C}$  by 50% (v/v) glycerol. The effect of the initial pH value of culture medium on the growth of *Leu. citreum* BH10 was shown in supplementary Fig. S1. The strain grew well when the pH value was 5.0~8.0.

The culture medium for exopolysaccharides production of *Leu. citreum* BH10 was composed of sucrose 180 g/L, peptone 10 g/L,  $\text{K}_2\text{HPO}_4$  5 g/L and sodium chloride 2 g/L. The mediums were sterilized at  $121^{\circ}\text{C}$  for 20 min before the experiment. The produced exopolysaccharide was named LCEPS.

### Optimization of LCEPS biosynthesis

Through creating second-order polynomial models in response surface methodology (RSM), the interactions and optimum conditions of variables for the desired response were studied and obtained. The effects of culture conditions on LCEPS production ( $Y_1$ ), including fermentation time ( $X_1$ ) (46 h, 48 h and 50 h), fermentation temperature ( $X_2$ ) ( $23^{\circ}\text{C}$ ,  $25^{\circ}\text{C}$  and  $27^{\circ}\text{C}$ ), sucrose concentration ( $X_3$ ) (18, 20 and 22%) and inoculation amount ( $X_4$ ) (1, 2 and 3%) were investigated (Fig. 1). A central composite design (CCD) with four variables were used to determine the optimum conditions for LCEPS biosynthesis. Each variable's low, middle and high levels were designated as  $-1$ ,  $0$  and  $1$ , respectively (Table 1). There were 30 experimental runs to be performed in a randomized form to obtain the optimal culture condition for *Leu. citreum* BH10, as well as to minimize the residual errors and effects of un-predicted variability from the systematic trends in the variables for the chosen responses under investigation (Chen et al. 2017; Karim

et al. 2014). These experiments included three replicates at center points. The RSM-CCD mathematical model and response surface 3D plots were established by Design-Expert software version 9.0 (Stat-Ease, Inc., Minneapolis, USA) to obtain the optimum conditions and graphical analysis of obtained data for the preparation of LCEPS.

### Preparation and characterization of LCEPS

#### LCEPS extraction

The 2% (v/v) activated *Leu. citreum* BH10 strain was inoculated into exopolysaccharides-producing medium and cultured at  $25^{\circ}\text{C}$  for 48 h (Abid et al. 2020; Bai et al. 2020). The fermentation broth was boiled in  $100^{\circ}\text{C}$  water-bath for 10 min to remove the likely enzymes degrading polysaccharides, cooled to room temperature, and then centrifuged at  $8,000\times g$  for 40 min at  $4^{\circ}\text{C}$  to remove bacterial impurities. Triplicate volumes of pre-cooled absolute ethanol (95% v/v) were added into the fermentation broth after cell removal, stirred following addition; the polysaccharide precipitation would slowly precipitate from the solution. The fermentation broth was set at  $4^{\circ}\text{C}$  overnight and then centrifuged at  $12,000\times g$  for 50 min at  $4^{\circ}\text{C}$ , the supernatant was discarded and polysaccharide precipitation was collected. Subsequently, the polysaccharide precipitation was dissolved with deionized water, then added with 80% (w/v) trichloroacetic acid solution to make the final concentration up to 5% (w/v). The mixed solution was stirred at room temperature for 2 h or set at  $4^{\circ}\text{C}$  overnight, then centrifuged at  $12,000\times g$  for 50 min at  $4^{\circ}\text{C}$  to remove the protein precipitation.

Triplicate volumes of pre-cooled absolute ethanol (95% v/v) were added to the supernatant again to obtain polysaccharide precipitation by centrifugation ( $12,000\times g$ ,  $4^{\circ}\text{C}$ , 40 min). The precipitation was dissolved in deionized water and put into the dialysis bags (8,000–14,000 Da) for dialysis for 48 h to remove small molecular substances. The LCEPS was obtained after concentration and freeze-drying.

#### Chemical and monosaccharide composition analysis

According to the methods reported by Rani et al. (2017), the content of protein, carbohydrate, uronic acid, and sulfate group was measured, respectively.

The monosaccharide composition of LCEPS was detected by HPLC as described previously (You et al. 2020). Firstly, the LCEPS (5.00 mg) sample and monosaccharide standards were hydrolyzed by 2 M trifluoroacetic acid (TFA) at  $120^{\circ}\text{C}$  for 2 h. Superfluous TFA was removed by distillation with methanol over three times. Then PMP derivatization was performed to convert the obtained hydrolyzate into its derivatives. Subsequently, the hydrolyzate was filtered through a  $0.22\mu\text{m}$

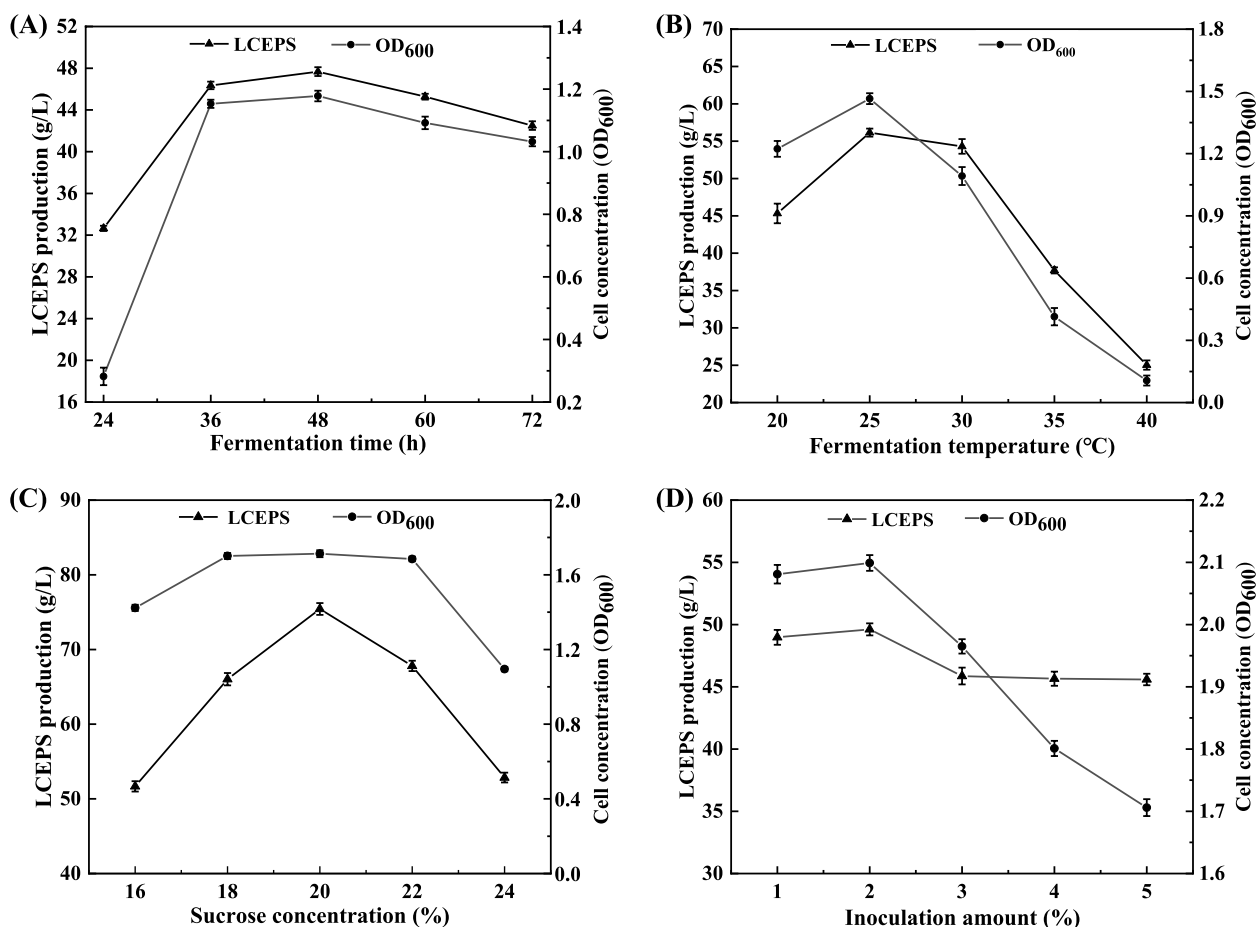


**Fig. 1** Effects of fermentation time, fermentation temperature, sucrose concentration and inoculation amount on the growth of *Leu. citreum* BH10 and the production of LCEPS

membrane and injected into the Waters LC-20A HPLC system (Tokyo, Japan) equipped with a Waters 2998 photodiode array detector at 250 nm and an EclipsePlus C18 column (4.6 × 250 mm, 5 μm) at 25 °C. The mobile phase was comprised of 0.1 M ammonium acetate (pH 7.0), acetonitrile and tetrahydrofuran with a ratio of 81:17:2 (v/v). The flow rate was set at 1.0 mL/min. By comparing the peak time and area of monosaccharide standards to determine the monosaccharide composition of LCEPS samples.

**Table 1** Variables and design levels for the CCD independent variables

Factor	Code	Level		
		-1	0	+1
Fermentation time (h)	X <sub>1</sub>	46	48	50
Fermentation temperature (°C)	X <sub>2</sub>	23	25	27
Sucrose concentration (%)	X <sub>3</sub>	18	20	22
Inoculation amount (%)	X <sub>4</sub>	1	2	3

**Mw and homogeneity determination**

The Mw and homogeneity of LCEPS were measured by gel permeation chromatography (GPC, Wyatt Technology Co., Ltd., Seattle, USA). Standard dextrans were injected into a Shodex OHpak series SB-806 HQ column (4.6 × 250 mm). The column was eluted with deionized water containing 0.02% (w/v) NaN<sub>3</sub> at a flow rate of 1.0 mL/min with a constant temperature of 40 °C. The elution volumes were plotted based on the logarithms of their respective molecular weights. About 2.00 mg/mL LCEPS solution was injected into the same operating system, and the elution volume was plotted in the same graph to determine the molecular weights.

**UV-vis and FT-IR spectra**

The UV-vis spectrum of LCEPS (0.50 mg/mL) was detected in the wavelength range of 190–500 nm by UV-1603 spectrophotometer (Shimadzu Co., Ltd. Kyoto, Japan). The FT-IR spectrum was performed in the wavelength range of 4000–500 cm<sup>-1</sup> by a Nicolet 6700

*FT-IR* spectra (Thermo Electron Co., Madison, USA). 1 mg of LCEPS sample was mixed with dried KBr powder (100 mg) and pressed into 1 mm pellets for *FT-IR* measurement (Wang, Li, Rui, et al. 2015c).

#### SEM observation of LCEPS

The LCEPS sample was glued onto aluminum stubs and then gold-sputtered. The microscopic surface morphology of it was observed by SEM (JEOL/EO, and model JSM-6380, Japan) at an accelerating voltage of 10 kV (Girard & Schaffer-Lequart 2008).

#### The $\zeta$ potential and particle size

The samples were determined by Marvin Zetasizer Nano ZSE  $\zeta$  potential and particle size analyzer (Marvin PANalytical Co., Ltd., UK) at 25 °C. The LCEPS solution was centrifuged at 12,000 × g for 40 min and filtered with 0.45 μm cellulose membrane. The instrument was set to automatic scanning mode, and each sample was measured for three times. The relationship between the  $\zeta$  potential and particle size of LCEPS solution with different concentrations was compared and analyzed (Omar-Aziz et al. 2020).

#### Thermodynamic properties of LCEPS

The determination was performed in a sealed manner to determine the melting point and enthalpy change of LCEPS by a differential scanning calorimeter (Netzsch STA449F3). The 7.36 mg of LCEPS sample was placed in an aluminum pan and an empty pan without samples was set as a reference. The sample was heated from 20 °C to 800 °C at 10 °C/min, keeping the airflow rate at 50 mL/min. The system used indium as the melting standard, and temperature readings were initially calibrated as described by Iftikhar et al. (2020) and Yang et al. (2018).

#### Emulsifying properties

The emulsifying property of LCEPS was analyzed according to the method described by Wang et al. (2021). About 0.5 mg of freeze-dried LCEPS, xanthan gum, gellan gum and sodium alginate were weighed and dissolved entirely in 0.5 mL deionized water. Subsequently, each solution was boiled for 20 min in a water bath and cooled to 25 °C. The phosphate buffer solution (PBS) was added to adjust the volume of each solution up to 2 mL. The solution was fully mixed by vortex vibration (constant volume) for 10 min after adding 0.5 mL cetane. Immediately after that, the absorbance value of the solution at 540 nm wavelength was read and recorded as  $A_0$ . Each solution sample was placed in sequence at 25 °C for 30, 60, and 90 min, and the corresponding absorbance value at 540 nm ( $A_t$ ) was recorded. Meanwhile, 2 mL PBS phosphate buffer and 0.5 mL cetane mixed solution were set

as the blank control. The emulsifying capacity of the sample was calculated according to the following formula, and expressed by the ratio of the absorbance value of the emulsion in the set time.

$$E = \frac{A_t}{A_0} * 10$$

#### Antioxidant properties of LCEPS

The 1.0 mL LCEPS solution (0.125–4.0 mg/mL) and 2.0 mL deionized water were sequentially added into 0.2 mL ethanolic DPPH radical solution (0.4 mM), fully mixed and placed in the dark at room temperature for 30 min. The absorbance was read at 517 nm. The scavenging rate of DPPH radical (%) =  $[1 - (A_{\text{sample}} - A_0) / A_{\text{blank}}] \times 100$ , where  $A_0$  represented the absorbance of the sample under identical condition as  $A_{\text{sample}}$  with water instead of DPPH radical solution, and deionized water and VC were used as the blank and positive control, respectively (Dilna et al. 2015; Moretto et al. 2021).

The hydroxyl radical was generated when 1 mL 0.75 mM  $\text{FeSO}_4$ , 1 mL 0.75 mM 1,10-phenanthroline, 1.5 mL 0.15 M sodium phosphate buffer (pH 7.4), and 1 mL  $\text{H}_2\text{O}_2$  (0.01%, v/v) were mixed. Then, the mixture was added with 1.0 mL sample solution (0.125–4.0 mg/mL) and incubated at 37 °C for 30 min. The absorbance of the mixture was read at 536 nm. The hydroxyl radical scavenging rate (%) =  $[(A_{\text{sample}} - A_{\text{blank}}) / (A_0 - A_{\text{blank}})] \times 100$ , where  $A_0$  represented the absorbance of the deionized water in the assay system excluding  $\text{H}_2\text{O}_2$  and sample, VC and deionized water were used as the positive control and blank, respectively (Tang et al. 2017).

Based on the method of Li et al. (2014), the superoxide radical scavenging activity was evaluated. When the 0.1 M sodium phosphate buffer (pH 7.4) containing 20 mM PMS, 156 mM NADH, and 52 mM NBT was prepared, the superoxide radical arose in the mixture. Then, the mixture was added with 1.0 mL sample solution (0.125–4.0 mg/mL) and incubated for 5 min at 25 °C. The absorbance of the mixture was determined at 560 nm. The superoxide radical scavenging rate (%) =  $(1 - A_{\text{sample}} / A_{\text{blank}}) \times 100$ . VC and deionized water were used as the positive control and blank, respectively.

#### Antibiofilm activities of LCEPS

##### Determination of planktonic growth

According to the method recommended by the Clinical and Laboratory Standards Institute, USA (2006), the effect of LCEPS on planktonic growth of the pathogens *S. aureus* ATCC 6538 was determined. Briefly, different amounts of LCEPS were dissolved in LB broth to prepare different concentrations with ranging from 0.125 to 8 mg/mL. Then,

150  $\mu$ L bacterial suspension ( $\sim 10^5$  CFU/mL) was added into 96-well plates, incubated for 30 h at 37°C, and monitored by Bioscreen C Automated Microbiology Growth Curve Analysis System (ALT, USA). Besides, the biomass of *S. aureus* ATCC 6538 in the broth added with different concentrations of LCEPS was determined. Firstly, 1% of tested pathogens (0.6 OD<sub>600</sub> nm) were inoculated to LB broth containing different concentrations of LCEPS ranging from 0.125 mg/mL to 8 mg/mL and cultured at 37°C for 48 h. The biomass of the total viable pathogens was measured by the plate count method (Zhang et al. 2014).

#### Determination of antibiofilm activities

The biofilm inhibition activity of LCEPS was performed based on the previous method (Zhang et al. 2020). The *S. aureus* ATCC 6538 strains were inoculated to LB broth at the ratio of 1:100, cultured overnight, and the obtained culture was added to a 96-well plate in equal proportion. Different concentrations of LCEPS components (0.125, 0.25, 0.5, 1.0, 2.0, 4.0, and 8.0 mg/mL) were prepared with sterile LB broth, filtered through a 0.22  $\mu$ m membrane and added into culture suspensions. The LB broth was added into wells and set as the negative control. Then, the plate was covered and incubated aerobically at 37°C for 24 h. Subsequently, the plate was gently rinsed with sterile normal saline to remove the bacteria that did not adhere. The remaining bacteria were fixed with 95% (v/v) methanol, and the plate was dried naturally. Then, each well was stained with 0.2 mL of 2% (w/v) crystal violet for 5 min. The excessive dyes were removed with sterile distilled water to wash the plate three times. After air drying naturally, 0.16 mL of 33% (v/v) glacial acetic acid was used to resolubilize the dyes bound to the adherent cells. The dissolved dye from each well (125  $\mu$ L) was diluted and equivalently transferred to the separation well in the optically transparent 96-well plate, and the value of OD was determined at 595 nm. The inhibition rate was based on the formula: Inhibition rate of biofilm formation (%) =  $[1 - (\text{OD}_{\text{assay}} / \text{OD}_{\text{control}})] \times 100\%$ .

#### In situ observation of biofilm by CLSM

The biofilms were observed under the non-destructive living cell laser confocal microscope imaging system (Ultra View VOX 3D, Perkin, Elmer, Germany) as described previously with modification (Yin et al. 2021). Firstly, 1% of an overnight culture of the tested bacteria was inoculated to fresh LB broth supplemented with or without LCEPS (8 mg/mL). Secondly, about 2 mL cell suspensions were dispensed into a 25 mm confocal dish. After incubation at 37°C for 48 h, the confocal dishes were carefully washed with PBS, stained with 10  $\mu$ g/mL DAPI (4,6-Diamidino-2-phenylindole dihydrochloride) staining solution and then observed by CLSM.

#### Statistical analysis

All measurements in this study were conducted in triplicates. The analysis of variance (ANOVA) was applied to establish the linear, quadratic, and interaction effects of the independent variables on the responses (LCEPS production). Various statistical parameters such as coefficient of determination ( $R^2$ ), adjusted coefficient of determination (adjusted  $R^2$ ), coefficient of variation (CV), and adequate precision were used to evaluate the adequacy and precision of the developed models. Significance of the responses was measured at  $p < 0.05$  and  $p < 0.01$  significant levels. IC<sub>50</sub> value was calculated by linear regression through IBM SPSS Statistics Software 25.0 version.

## Results and discussion

#### Building of regression model

The RSM was utilized to regulate the independent variables of fermentation time, fermentation temperature, sucrose concentration, and inoculation amount to increase LCEPS production, and the experimental results were shown in Table 2. The LCEPS production ( $Y_1$ ) was ranged from 36.55 g/L to 56.39 g/L. Based on the multiple regression analysis, the relationship between the four independent variables and LCEPS production ( $Y_1$ ) as a response was related to Eq. (1). Negative sign represents the antagonistic effect. In contrast, the positive sign in front of the terms represents synergistic effect (Chen et al. 2017).

$$Y_1 = 48.58 + 1.97X_1 + 1.60X_2 + 2.85X_3 + 2.98X_4 + 0.84X_1X_2 - 0.96X_1X_3 + 1.18X_1X_4 + 1.17X_2X_3 - 0.90X_2X_4 + 0.39X_3X_4 + 0.81X_1^2 - 5.34X_2^2 - 1.43X_3^2 - 0.17X_4^2 \quad (1).$$

$X_1$ ,  $X_2$ ,  $X_3$  and  $X_4$  were referred to as the coded values of fermentation time, fermentation temperature, sucrose concentration and inoculation amount, respectively.

The results of ANOVA, model adequacy and regression coefficients were presented in Table 3. The F-value of 37.89 and a  $p$ -value  $< 0.0001$  confirmed the significance of the model, whereas the lack of fit with  $p = 0.3159$  was not significant. The coefficient of determination ( $R^2$ ) value was 0.9997 and the adjusted  $R^2$  was 0.9903, indicating that the model was highly significant. Furthermore, the regression coefficients' values were close to 1, suggesting excellent correlations between predicted and true values (Hamid et al. 2016; Masoumi et al. 2011).

As shown in Table 3, the second-order terms of fermentation temperature and sucrose concentration were presented  $p$ -value  $< 0.05$  ( $< 0.0001$  and 0.0248, respectively) through ANOVA analysis, whereas that of fermentation time and inoculation amount was showed  $p$ -value  $> 0.05$  (0.3191 and 0.8254, respectively), indicating the two variables' second-order terms were not significant, but their linear terms were statistically significant. Besides, the  $p$ -values for  $X_1X_4$  and  $X_2X_3$  were less than 0.05 (0.0237 and 0.0401, respectively), suggesting obvious

**Table 2** Experimental design matrix and results

Number	Factor				LCEPS production actual value/ (g/L)	LCEPS production predictive value/ (g/L)
	Fermentation time (h) $X_1$	Fermentation temperature (°C) $X_2$	Sucrose concentration (%) $X_3$	Inoculation amount (%) $X_4$		
1	-1	-1	0	-1	44.59	43.86
2	-1	0	-1	1	41.81	43.42
3	-1	1	1	0	45.84	46.39
4	-1	-1	0	-1	38.96	38.45
5	0	0	0	0	46.92	48.58
6	-1	-1	-1	1	40.06	39.40
7	-1	0	1	1	51.99	51.82
8	-1	0	0	1	49.13	49.05
9	0	1	-1	0	40.30	39.39
10	0	1	1	1	48.35	46.75
11	0	1	-1	-1	37.51	37.52
12	0	0	0	0	47.73	48.58
13	0	-1	1	-1	38.11	37.46
14	0	-1	1	0	40.24	41.90
15	0	1	1	0	48.19	47.43
16	0	-1	0	0	41.45	41.64
17	0	1	0	0	45.28	44.84
18	1	1	0	1	49.87	51.55
19	1	-1	0	-1	38.01	38.35
20	1	-1	0	1	47.11	48.47
21	1	1	1	1	53.14	53.57
22	1	1	1	0	49.82	50.09
23	1	1	-1	-1	40.15	40.92
24	1	-1	-1	-1	36.55	36.59
25	1	0	1	0	52.35	51.82
26	1	0	1	1	55.96	56.20
27	1	0	-1	0	48.90	48.04
28	1	0	0	0	53.02	51.35
29	1	-1	1	1	49.19	48.16
30	1	0	0	1	56.39	55.34

interactions between the studied variables. To graphically visualize the interactions between the variables and their relationship with the response, three-dimensional (3D) response surface plots were generated (Fig. 2). Each figure presented the effect of two variables on LCEPS production when the other variables were kept at 0 levels within the studied experimental range.

The study was attempted to optimize the fermentation process to obtain the maximum LCEPS production. The results in Table 2 indicated the optimum conditions required for maximizing the response values. The predicted conditions required for obtaining the maximum LCEPS production (56.50 g/L) were 49.99 h, 25.59 °C, 21.66 and 3.00% for fermentation time, fermentation temperature,

sucrose concentration and inoculation amount, respectively. A high desirability level ( $D=1.0$ ) was obtained in the experiment. The results of the optimization were confirmed by the experimental data using treatment in three replicates with a mean of 55.96 g/L, which presented high matching between the experimental and predicted results. This confirmed the validity of RSM with good correlation.

#### Physicochemical properties of LCEPS

##### *The homogeneity, mw, chemical and monosaccharide composition of LCEPS*

The Mw of LCEPS was measured by GPC (Fig. 3A). As can be observed, its numerical average molecular weight

**Table 3** ANOVA for response surface quadratic models

Source	Sum of squares	df	Mean square	F value	p value	Significance
Model	942.93	14	67.35	37.89	< 0.0001	**
A	37.28	1	37.28	20.97	0.0004	**
B	31.51	1	31.51	17.72	0.0008	**
C	79.68	1	79.68	44.83	< 0.0001	**
D	69.67	1	69.67	39.19	< 0.0001	**
AB	6.17	1	6.17	3.47	0.0821	
AC	5.85	1	5.85	3.29	0.0897	
AD	11.26	1	11.26	6.34	0.0237	*
BC	8.98	1	8.98	5.05	0.0401	*
BD	5.92	1	5.92	3.33	0.0881	
CD	0.76	1	0.76	0.43	0.5241	
A <sup>2</sup>	1.89	1	1.89	1.06	0.3191	
B <sup>2</sup>	130.61	1	130.61	73.48	< 0.0001	**
C <sup>2</sup>	11.05	1	11.05	6.22	0.0248	*
D <sup>2</sup>	0.090	1	0.090	0.050	0.8254	
Residual	26.66	15	1.78			
Cor Total	26.34	14	1.88	5.79	0.3159	
Model	0.32	1	0.32			
Total deviation	969.59	29				
Correlation coefficient	R <sup>2</sup> = 0.9997			R <sup>2</sup> <sub>Adj</sub> = 0.9903		

Note: \*\* The difference was very significant ( $p < 0.01$ ); \* The difference was significant ( $0.01 < p < 0.05$ )

was large and computed to be  $8.99 \times 10^6$  Da, indicating the good viscosity of LCEPS. This was consistent with the results reported by Moghadam et al. (2019), which suggested that large Mw corresponded to fine viscosity. Besides, the contents of carbohydrates, uronic acid

and sulfate in LCEPS were about 74.56, 2.27 and 21.51%, respectively. No protein content was detected. And the retention time of referred monosaccharide standards was analyzed and compared with that of LCEPS (Fig. 3B), demonstrating that the LCEPS was comprised of glucose.

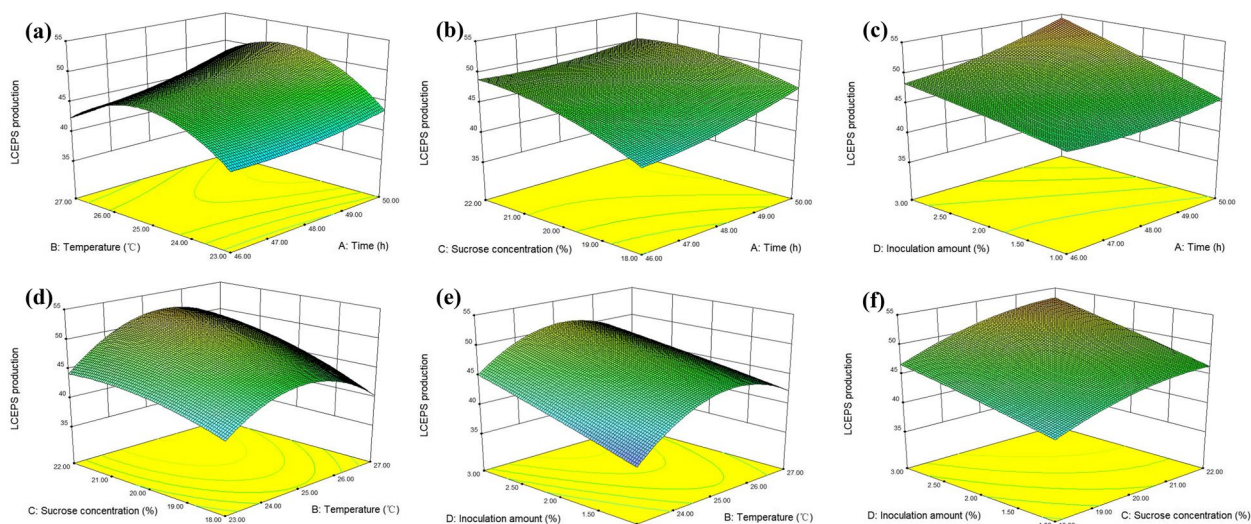


**Fig. 2** Response surface plots of LCEPS production as a function of fermentation temperature and fermentation time (a), sucrose concentration and fermentation time (b), inoculation amount and fermentation time (c), sucrose concentration and fermentation temperature (d), inoculation amount and fermentation temperature (e), and inoculation amount and sucrose concentration (f)



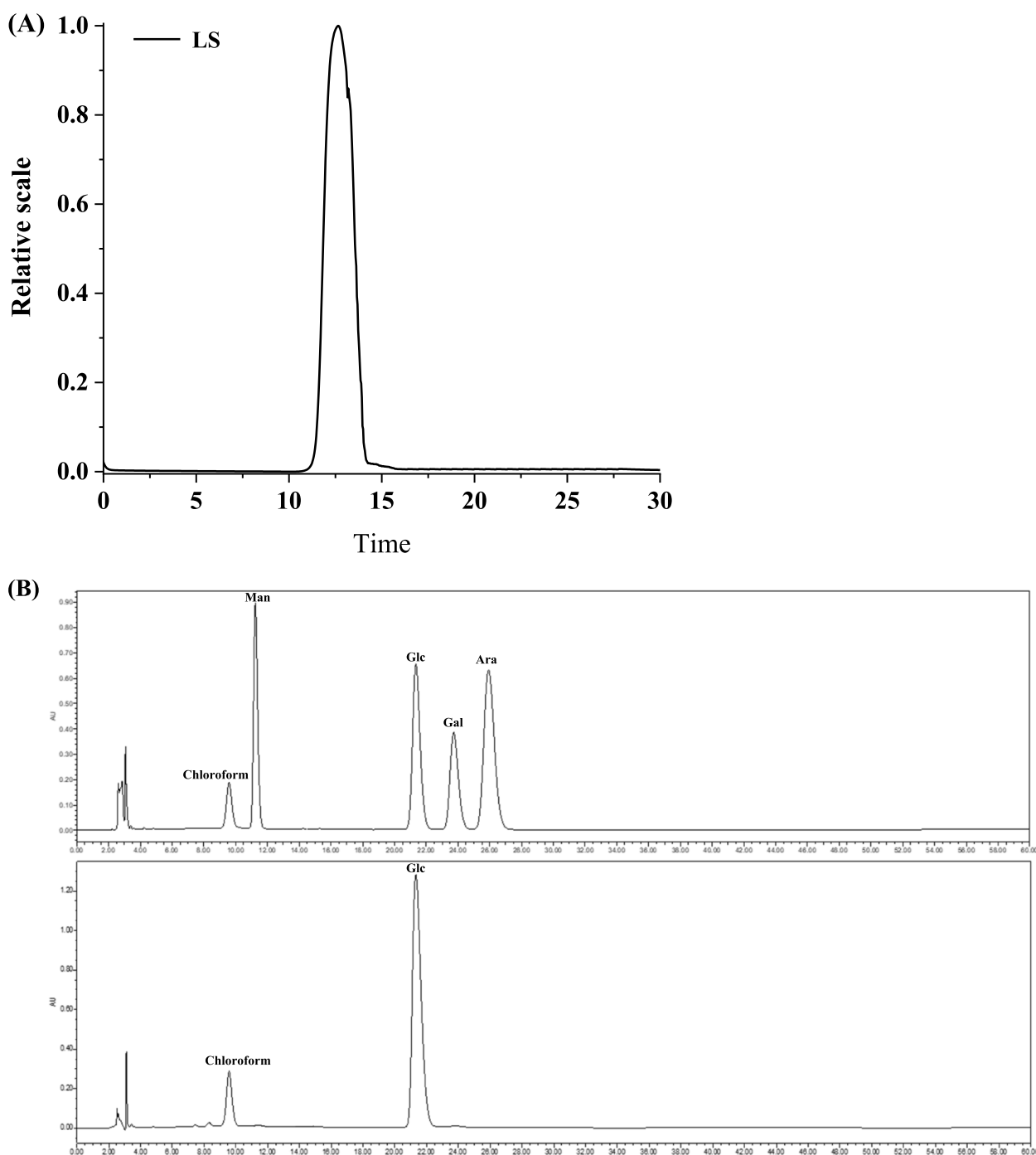


**Fig. 3** GPC chromatogram (A) and HPLC chromatogram (B) of LCEPS from *Leu. citreum* BH10. Man: mannose, Glc: glucose, Gal: galactose, Ara: arabinose

#### UV-vis and FT-IR spectra

The UV-vis spectrum of the LCEPS presented only a single peak at 210 nm. No other peak was discovered in 260–290 nm, which indicated that the LCEPS did not have any protein and nucleic acid (Fig. 4A).

The FT-IR spectrum of the LCEPS presented a strong and broad absorption at  $3315.44\text{ cm}^{-1}$ , indicating that the LCEPS contained many hydroxyl groups (O-H) (Fig. 4B). The hydroxyl stretching vibration caused the spectral phenomenon (Liu et al. 2019; Wang

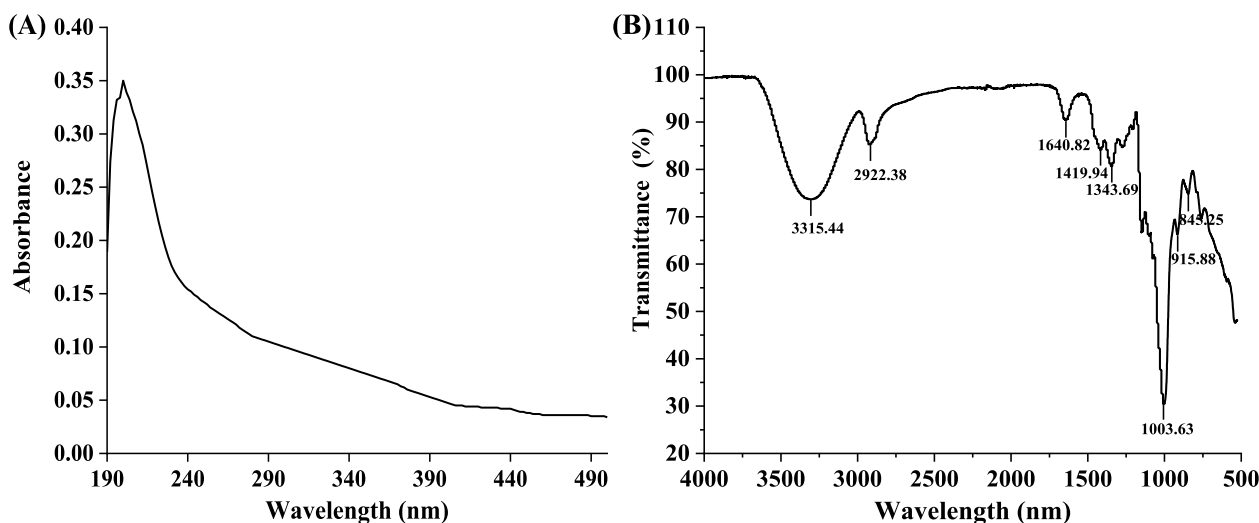


**Fig. 4** UV-vis (A) and FT-IR spectra (B) of LCEPS in the range 190–500 nm and 500–4000  $\text{cm}^{-1}$ , respectively

et al. 2019). The band at  $2922.38\text{cm}^{-1}$  was caused by the C-H stretching vibration (Rani et al. 2017; Zhang et al. 2016). The band at around  $1640.82\text{cm}^{-1}$  might be attributed to the existence of associated water. In the spectrum during  $1500\text{cm}^{-1}$ – $500\text{cm}^{-1}$ , the fine structure of LCEPS was reflected, the absorption peak at  $1419.94\text{cm}^{-1}$  and  $1343.69\text{cm}^{-1}$  were supposed to the C-O-C and C-O-H bond vibrations (Wang, Zhao, Tian, Yang, and Yang 2015). The infrared absorption peak at  $1003.63\text{cm}^{-1}$  was mostly caused by  $\alpha$ -(1 $\rightarrow$ 6) glycosidic bonds (Ye et al. 2012). The band at  $915.88\text{cm}^{-1}$  in the LCEPS was regarded as properties of pyranose ring stretching vibrations (Sran et al. 2019). Moreover, the band at  $845.25\text{cm}^{-1}$  was usually caused by  $\alpha$ -glycosidic bonds (Sirajunnisa et al. 2016). The results of monosaccharide composition and FT-IR spectra analysis indicated that the LCEPS was probably a homopolysaccharide and contained  $\alpha$ -type glycosidic bond to pyranose.

#### Observation of surface microscopic morphology

The surface morphology of LCEPS, xanthan gum and gellan gum were observed by SEM at 100 $\times$ , 1000 $\times$  and 5000 $\times$  (Fig. 5). LCEPS was appeared to be a hollow porous structure with stacked flakes of polysaccharide at low power observation, xanthan gum appeared to be compact and folded with potholes, whereas gellan gum appeared folded and smooth glittering surface. At higher magnification of 1000 $\times$  and 5000 $\times$ , the surface of LCEPS was more uneven and rough compared with that of xanthan gum and gellan gum, indicating the higher viscosity and more substantial water holding capacity of LCEPS. The characteristics illustrated that

LCEPS could have the potential to be set as an additive for application in food and cosmetics industries as thickening, emulsifying, stabilizing and texturing agent (Yang et al. 2015; Yang et al. 2018).

#### The $\zeta$ potential and particle size

The difference between the external charge of polysaccharide molecules and the surrounding suspension can be reflected by  $\zeta$  potential. And it could reflect the electrostatic repulsion between polysaccharide molecules (Gahruie et al. 2020). When the concentration of LCEPS ranged from 0.0 to 2.0 mg/mL, the corresponding  $\zeta$  potential value changed from  $-4.37\text{mV}$  to  $-10.46\text{mV}$  (Fig. 6A). The average particle size of LCEPS in aqueous solution increased with LCEPS concentration as well, rising from 108.17 nm to 909.13 nm. The  $\zeta$  absolute value and particle size increased with the solution concentration, and the  $\zeta$  absolute value was always lower than 30 mV ( $p < 0.05$ ). This phenomenon may be related with the composition of LCEPS, chain connection mode, and the interaction between hydroxyl and carboxyl groups and water. Besides, in order to ensure the stability of the solution system, there is a strong interaction between the particles with a small amount of negative charge, the attraction is greater than the repulsion, resulting in the increase of the particle size of the solution. Moreover, solution polydispersion coefficient (PDI) is an index to measure whether the particles are uniformly distributed. When PDI is equal to 1, the particles are monodispersed (Zambrano-Zaragoza et al. 2011). The average PDI of the LCEPS solution was 0.700, indicating that LCEPS was a homogeneous polysaccharide, which was consistent with that of Selene-rich *Grifola Fiodosa* (PDI=0.206)

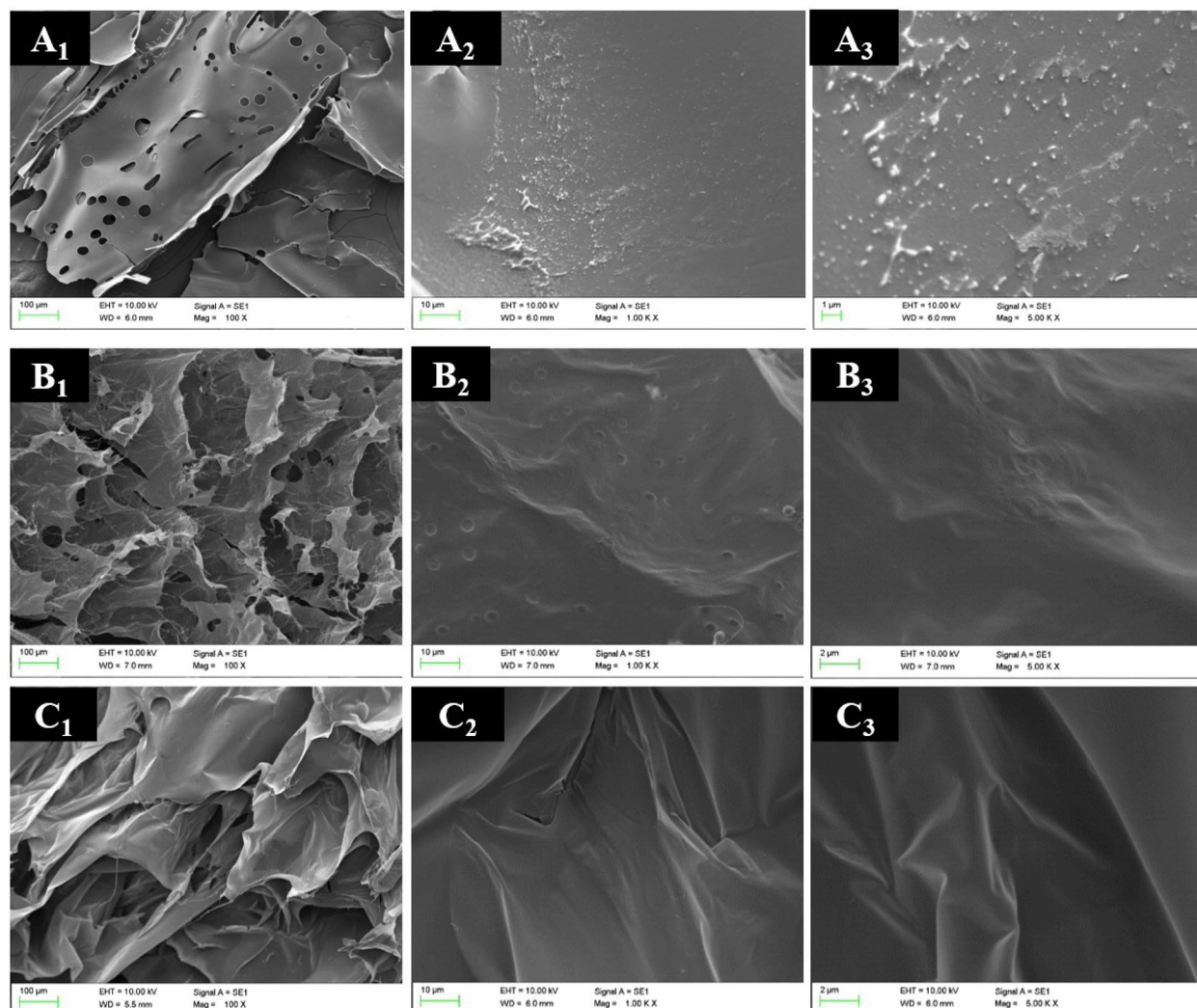


**Fig. 5** Surface morphology of the LCEPS (A), xanthan gum (B) and gellan gum (C) at various magnifications at 100 $\times$ , 1000 $\times$ , 5000 $\times$  by SEM

(Li et al. 2017). Taken together, these results indicated the possible application of LCEPS in high-concentration products.

#### Thermodynamic properties of LCEPS

The thermogravimetric analyzer was used to determine the thermodynamic properties of polysaccharide LCEPS (Fig. 6B). LCEPS had been losing weight ranging from the heating temperature of 33.19 $^{\circ}$ C to 793.10 $^{\circ}$ C. The TGA curve consisted of two distinct stages. In the first stage, from the initial temperature to 96.62 $^{\circ}$ C, the weight loss was nearly 8.00%, mainly because LCEPS contains many carboxyl groups, which can bind water molecules, and the temperature rise leads to the loss of bound water. Similarly, Wang et al. (2019) reported that a mass loss of approximately 9.7% PC EPS was observed between 43.9 $^{\circ}$ C and 99.7 $^{\circ}$ C. In

the second stage, from 96.62 $^{\circ}$ C to 793.10 $^{\circ}$ C, a weight loss of 77.97% was due to chemical reactions and changes in functional groups. When the temperature rose to 317.30 $^{\circ}$ C, half of the LCEPS weight was lost. The extrapolated starting and ending temperatures were 304.89 $^{\circ}$ C and 334.77 $^{\circ}$ C, respectively.

Differential scanning calorimetry (DSC) was used to analyze the changes in heat absorption and heat dissipation of LCEPS in the temperature rise process. The first and second endothermic peaks of EPS appeared at 73.33 $^{\circ}$ C and 243.42 $^{\circ}$ C, respectively (Fig. 6B). The initial temperature ( $T_0$ ), peak temperature ( $T_p$ ) and terminal temperature ( $T_c$ ) of the first endothermic peak were 73.33 $^{\circ}$ C, 130.42 $^{\circ}$ C and 155.68 $^{\circ}$ C, respectively. This stage was mainly related to the movement of bound water. The second endothermic peak was 260.61 $^{\circ}$ C to 323.74 $^{\circ}$ C, which was consistent with the

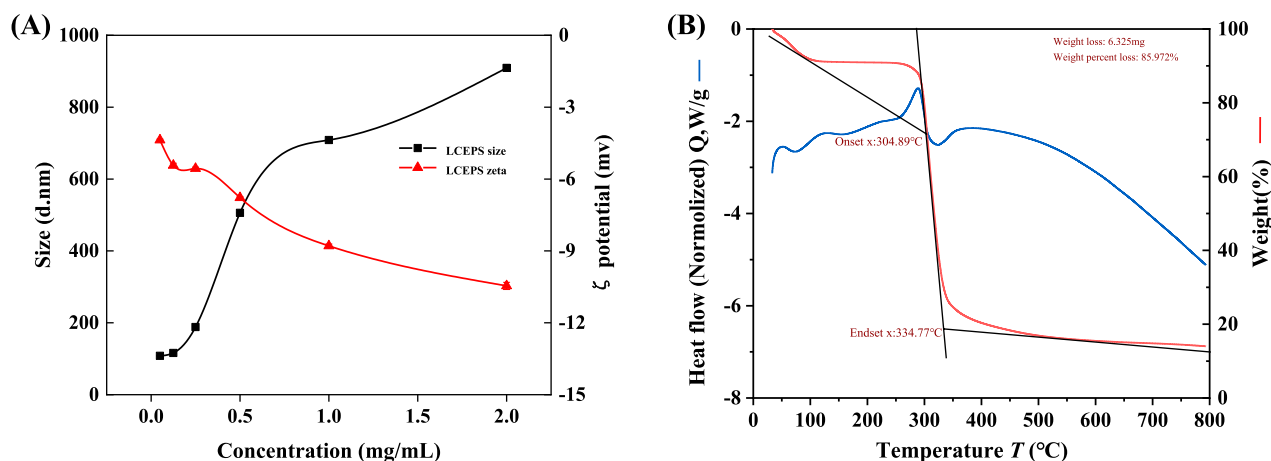


**Fig. 6** The ζ potential and particle size of LCEPS at various concentrations (A). TGA and DSC curves of LCEPS (B)

TGA curve. The results illustrated the high thermal stability of LCEPS, indicating its potential to be utilized in thermal processing.

**Emulsifying properties**

Many polysaccharides produced by plants or microorganisms have been proven to present high emulsifying properties and were extensively applied in the food industry. At the initial stage of emulsion formation, its structure was easy to be destroyed, the OD values were

measured at 30min and 60min after emulsion formation can be effectively used to evaluate the stability of emulsion (Wang et al. 2014; Wang et al. 2021). The smaller change in emulsification retention rate with time indicates that the emulsification capacity is stronger. The emulsification retention rate of LCEPS was made comparison with commercial gellan gum, xanthan gum and sodium alginate (Table 4). The emulsification retention rates of LCEPS were  $70.01 \pm 0.04\%$  and  $46.02 \pm 0.11\%$ , which was similar to that of sodium

**Table 4** Emulsifying activities of LCEPS

Emulsifier	Incubation time (min)	OD <sub>540</sub>	Emulsifying activity (%)
Control	0	0.241 ± 0.013	100 ± 0.00
	30	0.148 ± 0.018	61.15 ± 0.06
	60	0.072 ± 0.014	30.23 ± 0.07
	90	0.041 ± 0.005	17.12 ± 0.02
Gellan gum	0	0.564 ± 0.012	100 ± 0.00
	30	0.393 ± 0.019	93.03 ± 0.04
	60	0.259 ± 0.061	84.82 ± 0.01
	90	0.221 ± 0.010	75.86 ± 0.08
Xanthan gum	0	0.587 ± 0.035	100 ± 0.00
	30	0.446 ± 0.023	75.99 ± 0.03
	60	0.435 ± 0.048	74.49 ± 0.01
	90	0.362 ± 0.028	61.82 ± 0.07
Sodium alginate	0	0.951 ± 0.008	100 ± 0.00
	30	0.884 ± 0.035	77.78 ± 0.06
	60	0.806 ± 0.027	61.56 ± 0.02
	90	0.721 ± 0.075	47.85 ± 0.01
LCEPS	0	0.499 ± 0.081	100 ± 0.00
	30	0.387 ± 0.011	70.01 ± 0.04
	60	0.296 ± 0.045	46.02 ± 0.11
	90	0.232 ± 0.028	39.21 ± 0.02

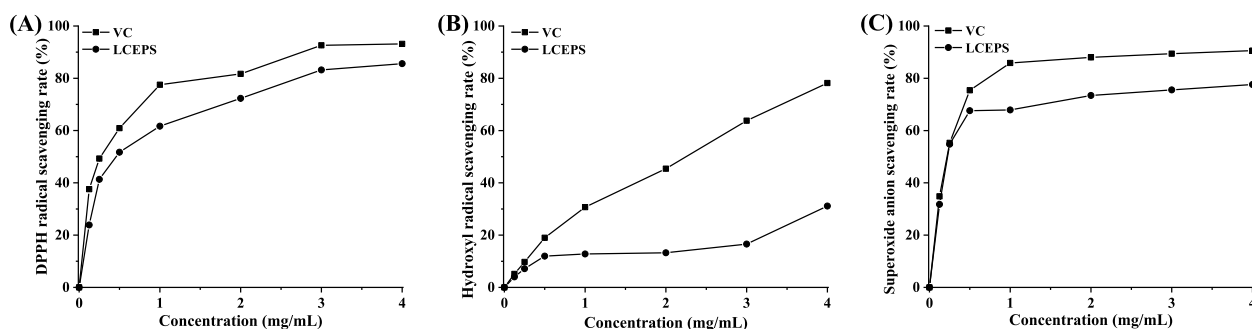


**Fig. 7** Scavenging activities on DPPH radical (A), hydroxyl radical (B) and superoxide radical (C) of LCEPS and VC

alginate were  $77.78 \pm 0.06\%$  and  $61.56 \pm 0.02\%$ , however, not as good as the emulsification retention rate of gellan gum ( $93.03 \pm 0.04\%$  and  $84.82 \pm 0.01\%$ ) and xanthan gum ( $75.99 \pm 0.03\%$  and  $74.49 \pm 0.01\%$ ). Besides, comparing the emulsification retention rate at 90 min, it was found that the emulsification retention rate of gellan gum was  $75.86 \pm 0.08\%$ , followed by xanthan gum ( $61.82 \pm 0.07\%$ ), and the emulsification retention rates of sodium alginate and LCEPS were  $47.85 \pm 0.01\%$  and  $39.21 \pm 0.02\%$ , respectively, indicating that the LCEPS produced by *Leu. citreum* BH10 could have the certain application value as an emulsification stabilizer.

**Antioxidant activities**

The DPPH, hydroxyl and superoxide radicals can promote the production of reactive oxygen species (ROS), leading to the reaction with biological macromolecules and causing aging, cancer, and other diseases (Chandrasekara et al. 2022; Liang et al. 2019; Yuan et al. 2017). In this study, VC and LCEPS showed great scavenging activity on DPPH radicals and superoxide radicals and

all presented dose-dependent manner from 0.125 mg/mL to 4 mg/mL (Fig. 7). The maximum DPPH scavenging activity was observed in VC (93.16%) and LCEPS (85.60%) at the concentration of 4 mg/mL (Fig. 7A), which was better than the DPPH scavenging activity of the EPS produced by *L. gasseri* FR4 (52.53%, 4 mg/mL) and *L. plantarum* C88 (75.95%, 4 mg/mL) (Rani et al. 2017; Zhang et al. 2013). The  $IC_{50}$  values of VC and LCEPS were 0.25 mg/mL and 0.48 mg/mL, respectively. Fig. 7B showed that the hydroxyl radical scavenging rate gradually increased with the increasing concentration of LCEPS, and the highest value scavenging rate could be up to 31.13% at 4 mg/mL, whereas VC reached 81.18% scavenging rate of hydroxyl radicals under corresponding concentration. The results were similar to the hydroxyl radical scavenging rate of EPS produced by *Leuconostoc citreum* B-2 and *Hirsutella sp* (Bai et al. 2020; Lei et al. 2015). And the  $IC_{50}$  values of VC and LCEPS were 1.83 mg/mL and 7.89 mg/mL, respectively, which were relatively higher than the  $IC_{50}$  values of DPPH scavenging activity. Besides, the  $IC_{50}$  values of VC and LCEPS to superoxide anion scavenging activity were 0.20 mg/mL and 0.25 mg/mL, respectively. The maximum superoxide anion scavenging activity of LCEPS was up to 77.63% at 4 mg/mL concentration (Fig. 7C), and the correspondingly scavenging activity of VC under the same concentration was 90.57%, which were both higher than that of EPS produced by *Lb. rhamnosus* (5.90% at 4 mg/mL) and *L. plantarum* YW32 (66.5%, 5 mg/mL) (Rajoka et al. 2017; Wang, Zhao, Yang, et al. 2015a). Taken together, the antioxidant assay results demonstrated that LCEPS has fine potential to be a free radical scavenger or inhibitor.

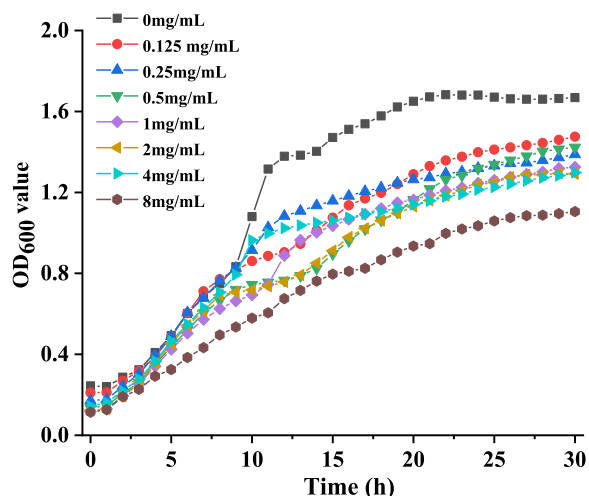


**Fig. 8** Growth of *S. aureus* ATCC 6538 in LB broth with LCEPS at concentrations of 0.125–8 mg/mL. Each value represented the average of triplicate independent assays

**Antibiofilm activities of LCEPS**

**Biofilm inhibition activity of LCEPS**

The effect of LCEPS on the growth of *S. aureus* ATCC 6538 was characterized by growth curve analysis (Fig. 8). The LCEPS exhibited no significant inhibitory effect on the growth of *S. aureus* ATCC 6538 at concentrations lower than 8 mg/mL. The inhibition ability of LCEPS

produced by *Leu. citreum* BH10 to biofilm-forming of foodborne pathogen bacteria *S. aureus* ATCC 6538 was investigated to evaluate its antibiofilm activities (Fig. 9A). The antibiofilm activity assay was set with varying concentrations of LCEPS (0.125–8.0 mg/mL). The inhibitory activities of the LCEPS on biofilm formation were dependent on concentration. The inhibition rate of LCEPS (8 mg/mL) on the biofilm formation of *S. aureus* ATCC 6538 reached  $38.43 \pm 1.45\%$ . Similarly, Zhang et al. (2020) reported the antibiofilm activities of anthocyanin-rich aqueous on *S. enterica* ATCC10398 was  $47.25 \pm 3.81\%$ . Besides, the LCEPS inhibited the biofilm formation of *S. aureus* ATCC 6538 without obvious biomass inhibition. Selvaraj et al. (2020) reported that *Sapindus mukorossi* methanolic extract (SMME) had antibiofilm without antibacterial effects. Some

studies demonstrated that the non-antibacterial activity of antibiofilm agents were considered more advantageous because it could exert any selective pressure on pathogenic bacteria and thus excludes the possibility of resistance development (Yin et al. 2021).

**In situ observation of *S. aureus* ATCC 6538 biofilms by CLSM**

The antibiofilm activity of the LCEPS could be directly observed by microscopic observation of pathogenic bacteria biofilm through invaluable insight by optical microscopy and CLSM z-section analysis (Fig. 9B). The images of the light microscopy and CLSM 2D images showed thinner and looser cell aggregates instead of typical biofilm architecture in the treatment groups with a concentration of 8 mg/mL LCEPS compared with the

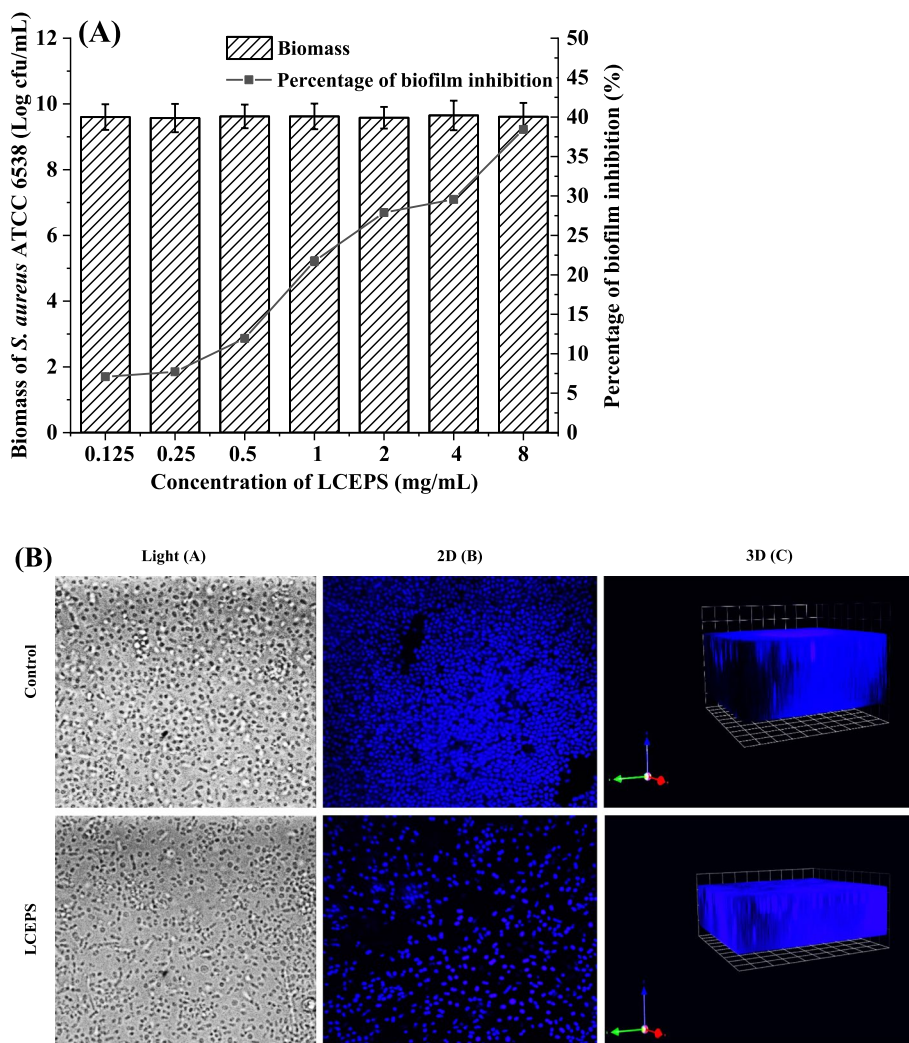


**Fig. 9** Effect of LCEPS on the biofilm inhibited percentage and biomass of *S. aureus* ATCC 6538 (A). CLSM observation of biofilm formation by *S. aureus* ATCC 6538 in the absence of LCEPS (Control) and the presence of LCEPS under light, 2D and 3D models (B)

control group without treatment. Furthermore, CLSM z-section analysis showed that the biofilms formed by the tested strains were compact when grown in the absence of LCEPS, whereas, in the LCEPS at 8 mg/mL test groups, a thinner and looser biofilm architecture and cell aggregates were observed. The confocal 3D images showed that the thicknesses of biofilms formatted by *S. aureus* ATCC 6538 in the negative control group were  $30.72 \pm 1.85 \mu\text{m}$ . However, when the *S. aureus* ATCC 6538 was incubated with 8 mg/mL LCEPS, the biofilm thicknesses dropped to  $17.53 \pm 1.05 \mu\text{m}$ . The development of biofilm is closely linked to the signal-mediated quorum sensing (QS) system, the formation of *S. aureus* biofilm may be effectively hindered by interference with QS (Galloway et al. 2012; Pang et al. 2019). The results demonstrated that the addition of LCEPS could effectively inhibit the formation of *S. aureus* ATCC 6538 biofilms, indicating that the LCEPS may potentially be developed as a new QS inhibitor and/or as food-grade adjuncts improve food safety.

## Conclusion

In the current study, the producing condition of LCEPS was optimized by RSM and LCEPS production was set as the response. The optimum condition was 49.99 h, 25.59 °C, 21.66 and 3.00% for fermentation time, fermentation temperature, sucrose concentration and inoculation amount, respectively, and the obtained LCEPS production was up to 55.96 g/L. The Mw of LCEPS was  $8.99 \times 10^6 \text{ Da}$ , and it was composed of glucose only. The high thermal properties of LCEPS indicated its potential to be used as an additive in hot processed foods. The fine emulsifying properties of LCEPS demonstrated that it could be used as a stabilizing and emulsifying agent. Besides, LCEPS presented specific antioxidant activity, especially through its strong scavenging ability of DPPH radicals. Moreover, LCEPS presented the fine ability to inhibit biofilm formation of foodborne pathogens, especially to *S. aureus* ATCC 6538. Hence, the excellent properties of LCEPS produced by *Leu. citreum* BH10 indicated its broad application prospects in food processing, pharmaceuticals and cosmetics.

## Abbreviations

LCEPS	Exopolysaccharides produced by <i>Leuconostoc citreum</i> BH10
EPS	Exopolysaccharides
GPC	Gel permeation chromatography
HPLC	High-performance liquid chromatography
Mw	Molecular weight
FT-IR	Fourier-transform infrared spectroscopy
UV-vis	Ultraviolet-visible
SEM	Scanning electron microscope
TGA	Thermogravimetric analysis
DSC	Differential scanning calorimetry
DAPI	4,6-Diamidino-2-phenylindole dihydrochloride
CLSM	Confocal laser scanning microscope
RSM	Response surface methodology

CCD	Central composite design
DPPH	2,2-diphenyl-1-picrylhydrazyl
NADH	Nicotinamide adenine dinucleotide
VC	Vitamin C
PMS	Phenazine metho-sulfate
NBT	Nitro blue tetrazolium
QS	Quorum sensing.

## Supplementary Information

The online version contains supplementary material available at <https://doi.org/10.1186/s43014-023-00134-3>.

**Additional file 1: Fig. S1.** Effects of initial pH value of culture medium on the growth of *Leu. citreum* BH10.

## Acknowledgments

Not applicable.

## Authors' contributions

Z. Ge: Formal analysis, Visualization, Writing-Original draft preparation. F. Azi: Writing-Review and Editing. X. Bao: Investigation, Software. X. Yin: Investigation, Validation. X. Feng: Conceptualization, Methodology. M. Zhang: Data curation, Software. X. Xia: Project administration, Supervision, Writing-Review and Editing. M. Dong: Conceptualization, Supervision, Fund acquisition, Writing-Review and Editing. All authors read and approved the final manuscript.

## Funding

This work was supported by the Fundamental Research Funds for the Central Universities (No. KYZZ2022001), Priority Academic Program Development of Jiangsu Higher Education Institutions (080-820830) and Jiangsu Agricultural Science and Technology Innovation Fund (Grant No. CX (21)2003).

## Availability of data and materials

All the data used to support the findings of this study are included in the article and in supplementary materials.

## Declarations

### Ethics approval and consent to participate

Not applicable.

### Consent for publication

Not applicable.

### Competing interests

The authors declare that they have no competing interests.

### Author details

<sup>1</sup>Institute of Agro-Product Processing, Jiangsu Academy of Agricultural Sciences, Nanjing 210014, China. <sup>2</sup>College of Food Science and Technology, Nanjing Agricultural University, Jiangsu Province, Nanjing 210095, China. <sup>3</sup>Jiangsu Key Laboratory for Food Quality and Safety-State Key Laboratory Cultivation Base, Ministry of Science and Technology, Nanjing 210014, China.

Received: 22 August 2022 Accepted: 10 January 2023

Published online: 02 May 2023

## References

- Abid, Y., Azabou, S., Blecker, C., Gharsallaoui, A., & Attia, H. (2020). Rheological and emulsifying properties of an exopolysaccharide produced by potential probiotic *Leuconostoc citreum* strain. *Carbohydrate Polymers*, 256(4), 117523. <https://doi.org/10.1016/j.carbpol.2020.117523>.
- Bai, M., Huang, T., Guo, S., Wang, Y., & Bilige, M. (2020). Probiotic lactobacillus casei Zhang improved the properties of stirred yogurt. *Food Bioscience*, 37, 100718. <https://doi.org/10.1016/j.fbio.2020.100718>.

- Chandrasekara, A., Senanayake, I., Kumari, D., & Shahidi, F. (2022). Effect of processing on the antioxidant activities of porridges and Pittu prepared from finger millets (Eleusine coracana). *Food Production, Processing and Nutrition*, 4(1), 1–14. <https://doi.org/10.1186/s43014-022-00097-x>.
- Chen, Y. W., Lee, H. V., & Hamid, S. B. A. (2017). Investigation of optimal conditions for production of highly crystalline nanocellulose with increased yield via novel Cr(III)-catalyzed hydrolysis: Response surface methodology. *Carbohydrate Polymers*, 178(12), 57–68. <https://doi.org/10.1016/j.carbpol.2017.09.029>.
- Dilna, V. S., Surya, H., Aswathy, R. G., Varsha, K. K., Sakthikumar, N. D., & Pandey, A. (2015). Characterization of an exopolysaccharide with potential health-benefit properties from a probiotic lactobacillus plantarum RIF(4). *LWT-Food Science and Technology*, 64, 1179–1186. <https://doi.org/10.1016/j.lwt.2015.07.040>.
- Enescu, C. M. (2017). Collection and use of birch sap, a less known non-wood forest product in Romania. *Sci Pap-Ser Manag Ec*, 17(1), 191–194. <https://doi.org/https://www.researchgate.net/publication/329962696>.
- Gahruie, H. H., Eskandari, M. H., Khalesi, M., Meeran, P. V., & Hosseini, S. M. (2020). Rheological and interfacial properties of basil seed gum modified with octenyl succinic anhydride. *Food Hydrocolloids*, 101, 105489. <https://doi.org/10.1016/j.foodhyd.2019.105489>.
- Galloway, W., Hodgkinson, J. T., Bowden, S., Welch, M., & Spring, D. R. (2012). Applications of small molecule activators and inhibitors of quorum sensing in gram-negative bacteria. *Trends in Microbiology*, 20(9), 449–458. <https://doi.org/10.1016/j.tim.2012.06.003>.
- Girard, M., & Schaffer-Lequart, C. (2008). Attractive interactions between selected anionic exopolysaccharides and milk proteins. *Food Hydrocolloids*, 22(8), 1425–1434. <https://doi.org/10.1016/j.foodhyd.2007.09.001>.
- Hamid, S., Chowdhury, Z. Z., Karim, M. Z., & Ali, M. E. (2016). Catalytic isolation and physicochemical properties of nanocrystalline cellulose (NCC) using HCl-FeCl<sub>3</sub> system combined with ultrasonication. *Bioresources*, 11(2), 3840–3855. <https://doi.org/10.15376/biores.11.2.3840-3855>.
- Iftikhar, R., Ansari, A., Siddiqui, N. N., Hussain, F., & Aman, A. (2020). Structural elucidation and cytotoxic analysis of a fructan based biopolymer produced extracellularly by *Zymomonas mobilis* KIBGE-IB14. *Carbohydrate Research*, 499, 108223. <https://doi.org/10.1016/j.carres.2020.108223>.
- Institute, C. L. S. (2006). Methods for dilution antimicrobial susceptibility tests for bacteria that grow aerobically. *Approved Standard*, M7, A7.
- Kallio, H., & Ahtonen, S. (1987). Seasonal variations of the sugars in birch sap. *Food Chemistry*, 25(4), 293–304. [https://doi.org/10.1016/0308-8146\(87\)90016-1](https://doi.org/10.1016/0308-8146(87)90016-1).
- Karim, M., Chowdhury, Z., Hamid, S., & Ali, M. (2014). Statistical optimization for acid hydrolysis of microcrystalline cellulose and its physicochemical characterization by using metal ion catalyst. *Materials*, 7(10), 6982–6999. <https://doi.org/10.3390/ma7106982>.
- Lei, M., Sun, S., Rong, L., Shen, Z., & Jiang, X. (2015). Antioxidant activity of polysaccharides produced by *Hirsutella* sp and relation with their chemical characteristics. *Carbohydrate Polymers*, 117, 452–457. <https://doi.org/10.1016/j.carbpol.2014.09.076>.
- Li, Q., Wang, W., Zhu, Y., Chen, Y., Zhang, W., & Yang, L. (2017). Structural elucidation and antioxidant activity a novel se-polysaccharide from se-enriched *Grifola frondosa*. *Carbohydrate Polymers*, 161(4), 42–52. <https://doi.org/10.1016/j.carbpol.2016.12.041>.
- Li, W., Ji, J., Rui, X., Yu, J. J., & Tang, W. Z. (2014). Production of exopolysaccharides by *Lactobacillus helveticus* MB2–1 and its functional characteristics in vitro. *LWT-Food Science and Technology*, 59, 732–739. <https://doi.org/10.1016/j.lwt.2014.06.063>.
- Liang, Y., Li, Y., Zhang, L., & Liu, X. (2019). Phytochemicals and antioxidant activity in four varieties of head cabbages commonly consumed in China. *Food Production, Processing and Nutrition*, 1(1), 1–9. <https://doi.org/10.1186/s43014-019-0003-6>.
- Liu, T., Zhou, K., Yin, S., Liu, S., & Wang, C. (2019). Purification and characterization of an exopolysaccharide produced by *Lactobacillus plantarum* HY isolated from home-made Sichuan pickle. *International Journal of Biological Macromolecules*, 134(8), 516–526. <https://doi.org/10.1016/j.ijbiomac.2019.05.010>.
- Masoumi, H. R. F., Kassim, A., Basri, M., & Abdullah, D. K. (2011). Determining optimum conditions for lipase-catalyzed synthesis of triethanolamine (TEA)-based esterquat cationic surfactant by a Taguchi robust design method. *Molecules*, 16(6), 4672–4680. <https://doi.org/10.3390/molecules16064672>.
- Moghadam, B. E., Keivaninahr, F., Nazemi, A., Fouladi, M., Mokarram, R., & Benis, K. Z. (2019). Optimization of conjugated linoleic acid production by *Bifidobacterium animalis* subsp. *Lactis* and its application in fermented milk. *LWT-Food Science & Technology*, 108, 344–352. <https://doi.org/10.1016/j.lwt.2019.03.071>.
- Moretto, L., Tonolo, F., Folda, A., Scalcon, V., & Rigobello, M. P. (2021). Comparative analysis of the antioxidant capacity and lipid and protein oxidation of soy and oats beverages. *Food Production Processing and Nutrition*, 3(1), 1–10. <https://doi.org/10.1186/s43014-020-00046-6>.
- Omar-Aziz, M., Yarmand, M. S., Khodajyan, F., Mousavi, M., Gharaghani, M., Kennedy, J. F., & Hosseini, S. S. (2020). Chemical modification of pullulan exopolysaccharide by octenyl succinic anhydride: Optimization, physicochemical, structural and functional properties. *International Journal of Biological Macromolecules*, 164(12), 3485–3495. <https://doi.org/10.1016/j.ijbiomac.2020.08.158>.
- Pang, Z., Raudonis, R., Bernard, R. G., Lin, T., & Cheng, Z. (2019). Antibiotic resistance in *Pseudomonas aeruginosa*: Mechanisms and alternative therapeutic strategies. *Biotechnology Advances*, 37(1), 177–192. <https://doi.org/10.1016/j.biotechadv.2018.11.013>.
- Rajoka, M. R., Jin, M., Haobin, Z., Li, Q., Shao, D., Shi, J., & Hussain, N. (2017). Functional characterization and biotechnological potential of exopolysaccharide produced by *Lactobacillus rhamnosus* strains isolated from human breast milk. *LWT-Food Science and Technology*, 89, 638–647. <https://doi.org/10.1016/j.lwt.2017.11.034>.
- Rani, R. P., Anandharaj, M., & A., D. R. (2017). Characterization of a novel exopolysaccharide produced by *Lactobacillus gasserii* FR4 and demonstration of its in vitro biological properties. *International Journal of Biological Macromolecules*, 109, 772–783. <https://doi.org/10.1016/j.ijbiomac.2017.11.062>.
- Selvaraj, A., Valliammai, A., Premika, M., Priya, A., Bhaskar, J. P., Krishnan, V., & Pandian, S. K. (2020). *Sapindus mukorossi* Gaertn. And its bioactive metabolite oleic acid impedes methicillin-resistant *Staphylococcus aureus* biofilm formation by down regulating adhesion genes expression. *Microbiological Research*, 242(1), 126601. <https://doi.org/10.1016/j.micres.2020.126601>.
- Sirajunnisa, A. R., Vijayagopal, V., Sivaprakash, B., Viruthagiri, T., & Surendhiran, D. (2016). Optimization, kinetics and antioxidant activity of exopolysaccharide produced from rhizosphere isolate, *Pseudomonas fluorescens* CrN6. *Carbohydrate Polymers*, 135(1), 35–43. <https://doi.org/10.1016/j.carbpol.2015.08.080>.
- Sran, K. S., Sundharam, S., Krishnamurthi, S., & Choudhury, A. R. (2019). Production, characterization and bio-emulsifying activity of a novel thermostable exopolysaccharide produced by a marine strain of *Rhodobacter johrii* CDR-SL 7Cii. *International Journal of Biological Macromolecules*, 127, 240–249. <https://doi.org/10.1016/j.ijbiomac.2019.01.045>.
- Tang, W., Dong, M., Wang, W., Han, S., Rui, X., Wu, J., & Li, W. (2017). Structural characterization and antioxidant property of released exopolysaccharides from *Lactobacillus delbrueckii* ssp. *bulgaricus* SRFM–1. *Carbohydrate Polymers*, 173(10), 654–664. <https://doi.org/10.1016/j.carbpol.2017.06.039>.
- Wang, B., Song, Q., Zhao, F., Xiao, H., Zhou, Z., & Han, Y. (2019). Purification and characterization of dextran produced by *Leuconostoc pseudomesenteroides* PC as a potential exopolysaccharide suitable for food applications. *Process Biochemistry*, 87(12), 187–195. <https://doi.org/10.1016/j.procbio.2019.08.020>.
- Wang, J., Zhao, X., Tian, Z., Yang, Y., & Yang, Z. (2015b). Characterization of an exopolysaccharide produced by *Lactobacillus plantarum* YW11 isolated from Tibet kefir. *Carbohydrate Polymers*, 125, 16–25. <https://doi.org/10.1016/j.carbpol.2015.03.003>.
- Wang, J., Zhao, X., Yang, Y., Zhao, A., & Yang, Z. (2015a). Characterization and bioactivities of an exopolysaccharide produced by *Lactobacillus plantarum* YW32. *International Journal of Biological Macromolecules*, 74, 119–126. <https://doi.org/10.1016/j.ijbiomac.2014.12.006>.
- Wang, K., Li, W., Rui, X., Chen, X. H., Jiang, M., & Dong, M. S. (2014). Characterization of a novel exopolysaccharide with antitumor activity from *Lactobacillus plantarum* 70810. *International Journal of Biological Macromolecules*, 63, 133–139. <https://doi.org/10.1016/j.ijbiomac.2013.10.036>.
- Wang, K., Li, W., Rui, X., Li, T., & Dong, M. (2015c). Chemical modification, characterization and bioactivity of a released exopolysaccharide (r-EPS1) from *Lactobacillus plantarum* 70810. *Glycoconjugate Journal*, 32(1–2), 17–27. <https://doi.org/10.1007/s10719-014-9567-1>.
- Wang, L., Gu, Y., Zheng, X., Zhang, Y., Deng, K., Wu, T., & Cheng, H. (2021). Analysis of physicochemical properties of exopolysaccharide from



- Leuconostoc mesenteroides strain XR1 and its application in fermented milk. *LWT-Food Science and Technology*, 146(7), 111449. <https://doi.org/10.1016/j.lwt.2021.111449>.
- Yang, Y., Feng, F., Zhou, Q., Zhao, F., Du, R., Zhou, Z., & Han, Y. (2018). Isolation, purification and characterization of exopolysaccharide produced by *Leuconostoc pseudomesenteroides* YF32 from soybean paste. *International Journal of Biological Macromolecules*, 114(7), 529–535. <https://doi.org/10.1016/j.ijbiomac.2018.03.162>.
- Yang, Y., Peng, Q., Guo, Y., Han, Y., Xiao, H., & Zhou, Z. (2015). Isolation and characterization of dextran produced by *Leuconostoc citreum* NM105 from manchurian sauerkraut. *Carbohydrate Polymers*, 133(11), 365–372. <https://doi.org/10.1016/j.carbpol.2015.07.061>.
- Ye, S., Feng, L., Wang, J., Wang, H., & Zhang, M. (2012). Antioxidant activities of an exopolysaccharide isolated and purified from marine *Pseudomonas* PF-6. *Carbohydrate Polymers*, 87(1), 764–770. <https://doi.org/10.1016/j.carbpol.2011.08.057>.
- Yin, L., Zhang, Y., Azi, F., Zhou, J., Dong, M., & Xia, X. (2021). Inhibition of biofilm formation and quorum sensing by soy isoflavones in *Pseudomonas aeruginosa*. *Food Control*, 133, 108629. <https://doi.org/10.1016/j.foodcont.2021.108629>.
- You, X., Li, Z., Ma, K., Zhang, C., & Li, W. (2020). Structural characterization and immunomodulatory activity of an exopolysaccharide produced by *Lactobacillus helveticus* LZ-R-5. *Carbohydrate Polymers*, 235(5), 115977. <https://doi.org/10.1016/j.carbpol.2020.115977>.
- Yuan, X., Li, L., Sun, H., Sun, S., & Zhang, Z. (2017). Optimization of subcritical water extraction of polysaccharides from *Inonotus obliquus* and their antioxidant activities. *International Journal of Biology*, 9(3), 38–50. <https://doi.org/10.5539/ijb.v9n3p38>.
- Zambrano-Zaragoza, M. L., Mercado-Silva, E., Gutierrez-Cortez, E., Castano-Tostado, E., & Quintanar-Guerrero, D. (2011). Optimization of nanocapsules preparation by the emulsion-diffusion method for food applications. *LWT-Food Science and Technology*, 44(6), 1362–1368. <https://doi.org/10.1016/j.lwt.2010.10.004>.
- Zhang, J., Cao, Y. Q., Wang, J., Guo, X. L., Zheng, Y., & Yang, Z. N. (2016). Physicochemical characteristics and bioactivities of the exopolysaccharide and its sulphated polymer from *Streptococcus thermophilus* GST-6. *Carbohydrate Polymers*, 146, 368–375. <https://doi.org/10.1016/j.carbpol.2016.03.063>.
- Zhang, J., Rui, X., Wang, L., Guan, Y., Sun, X., & Dong, M. (2014). Polyphenolic extract from *Rosa rugosa* tea inhibits bacterial quorum sensing and biofilm formation. *Food Control*, 42(8), 125–131. <https://doi.org/10.1016/j.foodcont.2014.02.001>.
- Zhang, L., Liu, C., Li, D., Zhao, Y., Yang, Z., & Li, S. (2013). Antioxidant activity of an exopolysaccharide isolated from *Lactobacillus plantarum* C88. *International Journal of Biological Macromolecules*, 54, 270–275. <https://doi.org/10.1016/j.ijbiomac.2012.12.037>.
- Zhang, Y., Lin, Y. F., Huang, L., Tekliye, M., Rasheed, H. A., & Dong, M. S. (2020). Composition, antioxidant, and anti-biofilm activity of anthocyanin-rich aqueous extract from purple highland barley bran. *LWT-Food Science and Technology*, 125, 109181. <https://doi.org/10.1016/j.lwt.2020.109181>.

## Publisher's Note

Springer Nature remains neutral with regard to jurisdictional claims in published maps and institutional affiliations.

Ready to submit your research? Choose BMC and benefit from:

- fast, convenient online submission
- thorough peer review by experienced researchers in your field
- rapid publication on acceptance
- support for research data, including large and complex data types
- gold Open Access which fosters wider collaboration and increased citations
- maximum visibility for your research: over 100M website views per year

At BMC, research is always in progress.

Learn more [biomedcentral.com/submissions](https://biomedcentral.com/submissions)

